Molecular and Cellular Biochemistry (2020) 470:63–75
https://doi.org/10.1007/s11010-020-03747-1

CIGB-300 anticancer peptide regulates the protein kinase CK2-dependent phosphoproteome

Yasser Perera[1,2] · Yassel Ramos[3] · Gabriel Padrón[3] · Evelin Caballero[2] · Osmany Guirola[3] · Lorena G. Caligiuri[4] · Norailys Lorenzo[4] · Florencia Gottardo[4] · Hernán G. Farina[4] · Odile Filhol[5] · Claude Cochet[5] · Silvio E. Perea[2]

Received: 13 January 2020 / Accepted: 6 May 2020 / Published online: 13 May 2020

Abstract

Casein-kinase CK2 is a Ser/Thr protein kinase that fosters cell survival and proliferation of malignant cells. The CK2 holoenzyme, formed by the association of two catalytic alpha/alpha' (CK2α/CK2α') and two regulatory beta subunits (CK2β), phosphorylates diverse intracellular proteins partaking in key cellular processes. A handful of such CK2 substrates have been identified as targets for the substrate-binding anticancer peptide CIGB-300. However, since CK2β also contains a CK2 phosphorylation consensus motif, this peptide may also directly impinge on CK2 enzymatic activity, thus globally modifying the CK2-dependent phosphoproteome. To address such a possibility, firstly, we evaluated the potential interaction of CIGB-300 with CK2 subunits, both in cell-free assays and cellular lysates, as well as its effect on CK2 enzymatic activity. Then, we performed a phosphoproteomic survey focusing on early inhibitory events triggered by CIGB-300 and identified those CK2 substrates significantly inhibited along with disturbed cellular processes. Altogether, we provided here the first evidence for a direct impairment of CK2 enzymatic activity by CIGB-300. Of note, both CK2-mediated inhibitory mechanisms of this anticancer peptide (i.e., substrate- and enzyme-binding mechanism) may run in parallel in tumor cells and help to explain the different anti-neoplastic effects exerted by CIGB-300 in preclinical cancer models.

Keywords CIGB-300 · CK2 · Anticancer peptides · CPP · Clinical-grade CK2 inhibitor · Phosphoproteomics

Introduction

Casein-kinase 2 (CK2) seems to account for about 20% of the cellular phosphoproteome in living cells [1]. This enzyme is usually deregulated in malignant cells and has been linked to hallmarks of cancer including exacerbated cell proliferation, increased survival, angiogenesis, and metastasis [2]. Of note, CK2 modulates the activity of substrates with driver roles in cancer including both tumor suppressors like PTEN [3] and PML [4], as well as oncogenes like AKT [5] and c-myc [6]. Moreover, aberrant CK2 expression impacts on several signaling pathways whose deregulation leads to malignant transformation including Wnt signaling, Hedgehog signaling (Hh), JAK/STAT, and PI3K/AKT pathway [7].

CK2 enzymatic activity is exerted by the catalytic subunits alone and/or the full holoenzyme which is composed of two catalytic CK2α/α' and two regulatory CK2β subunits [8]. Phosphorylation of a subset of substrates can only be exerted by the holoenzyme $CK2\alpha_2\beta_2$ (class-III substrates), whereas class-I substrates can be phosphorylated either by $CK2\alpha_2\beta_2$ or the free catalytic subunits. A third class of CK2

Electronic supplementary material The online version of this article (https://doi.org/10.1007/s11010-020-03747-1) contains supplementary material, which is available to authorized users.

✉ Yasser Perera
yasserperera@outlook.com

1 China-Cuba Biotechnology Joint Innovation Center (CCBJIC), Yongzhou Zhong Gu Biotechnology Co., Ltd, Yangjiaqiao Street, Lengshuitan District, Yongzhou City 425000, Hunan Province, China

2 Molecular Oncology Group, Division of Pharmaceuticals, Center for Genetic Engineering & Biotechnology, Ave 31 e/158 & 190, Playa, 10600 Havana, Cuba

3 Department of Proteomics. Biomedical Research Division, Center for Genetic Engineering & Biotechnology, Havana, Cuba

4 Platform of Biotechnology Services, Quilmes National University, Roque Saenz Peña 352, 1876 Bernal, Buenos Aires, Argentina

5 University of Grenoble Alpes, Inserm U1036, CEA, IRIG-BCI, 38000 Grenoble, France

substrates (class-II) is only phosphorylated by the catalytic subunits. Of note, the validity of such classification has been experimentally tested for a limited subset of recombinant CK2 substrates in cell-free assays [9].

CK2 is regarded as a promising druggable cancer target based on successful in vivo proof-*of*-concept using small molecule inhibitors that block either the ATP-binding site or antagonize the interaction between subunits [10, 11]. Additionally, antisense oligonucleotides that target the CSNK2A1 gene have shown to induce cell death and anti-tumoral activity [12]. However, only two compounds targeting the CK2-mediated phosphorylation have already entered into Clinical Trials: the ATP-competitive inhibitor CX-4945 and the CK2-substrate-targeting peptide CIGB-300 [13, 14].

The CIGB-300 peptide is a clinical-grade CK2 inhibitor that binds to the conserved CK2 phosphoacceptor site on CK2 substrates [15]. Among such, experimental findings in solid tumor-derived cell lines pointed out to the nucleolar protein B23/NPM1 as a major CIGB-300 target [16]. Subsequent pull-down experiments showed that the peptide binds a range of CK2 substrates [17]. Data from blood cancer cells further showed that phosphorylation of AKT and PTEN at CK2 target sites is also impaired [18]. These findings suggest that the array of CK2 substrates potentially inhibited by CIGB-300 in cancer may be diverse. One formal possibility not tested so far is that CIGB-300 impairs CK2β autophosphorylation. Since, CIGB-300 binds CK2 consensus sequence and CK2β contains such motif [19, 20], the peptide may also directly impinge on $CK2\alpha_2\beta_2$ enzymatic activity. CK2β autophosphorylation has been functionally associated with CK2 enzymatic activity, its intracellular stability, and the assembly of supra-molecular complexes of the enzyme [21, 22]. Thus, a direct and global CK2 enzymatic activity inhibition would explain the observed perturbation of disparate cellular processes like RNA processing, protein translation, proliferation/apoptosis, and cell adhesion in cells treated with this peptide [23].

Here, we demonstrated for the first time that CIGB-300 interacts with CK2α and blocks the enzymatic activity of $CK2\alpha_2\beta_2$ towards selected class-III substrates in cell-free assays. Such direct enzyme inhibition may run in parallel to the previously described inhibitory mechanism based on CIGB-300 binding to CK2 phosphoacceptor site [16]. Using a label-free phosphoproteomic approach, we address such complexity and provide evidence for a global impact of CIGB-300 on the CK2-mediated phosphoproteome in a model tumor cell. Furthermore, inferred from kinase-substrate relationships, we uncovered new potential targets for this peptide and identified perturbed biological processes. Rather than using iteratively low-throughput experiments to identify the full array of CK2 substrates impaired by CIGB-300, we performed a phosphoproteome profiling to obtain a global glimpse of perturbed proteins and related pathways. Furthermore, although this is not a head-*to*-head experiment, our study provides a framework to globally compare two clinically relevant CK2 inhibitors with different mechanisms of action, i.e., CX-4945 and CIGB-300.

Methods and materials

Cell lines

The non-small cell lung cancer (NSCLC) cell line NCI-H125, kindly provided by Dr. Eduardo Suarez (Center for Molecular Immunology, Havana, Cuba), was originally obtained from ATCC (Rockville, MD). The NCI-H125 cells were cultured in RPMI 1640 (Life Technologies, USA) and supplemented with 10% fetal bovine serum (FBS; PAA, Canada) and 100 µg/mL gentamicin (Sigma, USA) at 37 °C in a humidified atmosphere containing 5% CO_2.

Synthetic peptides

CIGB-300 and canonical peptide substrates 29 (RRREDEESDDEE) and M (MSGDEMIFDPTMSKKKKKKKKP) were synthesized on solid phase and purified by RP-HPLC to > 98% purity on acetonitrile/H2O-trifluoroacetic acid gradient and confirmed by ion-spray mass spectrometry (Micromass, Manchester, UK).

Recombinant proteins

GST-Olig2, GST-Six1, and GST-CK2α fusion proteins were expressed and further purified by glutathione sepharose 4B GST-tagged protein purification resin. Calmodulin was purchased from Abcam (ab94519). Maltose Binding Protein (MBP)-CK2β subunit was obtained as previously described [24].

CK2 phosphorylation assays

A radiometric CK2 assay was performed in a final volume of 18 µL containing increasing concentrations of CIGB-300 or equivalent amount of dimethyl sulfoxide (DMSO) as control, 3 µL of CK2α (28 ng) or the holoenzyme, and a mixture containing 1 mM of the peptide substrates (M or 29), 10 mM $MgCl_2$, and 100 mM [γ-32P]-ATP (6000 Ci/mmol). Assays were performed at room temperature for 5 min before termination by the addition of 60 µL of 4% trichloroacetic acid. Additionally, recombinant CK2 protein substrates were incubated with CK2α (26 ng) in the absence or presence of CK2β (52 ng) and the phosphorylation was carried out in the presence of increasing concentrations of CIGB-300. In another experimental setting, CK2α (26 ng) was incubated with increasing amounts of CK2β in the absence or presence

of 100 μM CIGB-300; then the CK2 activity was assayed with peptide M substrate. Finally, in a fourth experimental setting, GST-CK2α (80 ng) was incubated for 30 min in the absence or presence of 50 μM CIGB-300; then the fusion protein was adsorbed on Glutathione-Sepharose beads; after washing, the beads were incubated with 160 ng CK2β and CK2 activity was assayed with peptide substrate M. Phosphoproteins were analyzed by SDS-PAGE followed by Coomassie staining and autoradiography and ^{32}P incorporation was quantified using Bio1D.

For the CK2β autophosphorylation assay, CK2α (120 ng) was incubated with CK2β (240 ng) and the reaction was carried out in the presence of increasing concentrations of CIGB-300. Autophosphorylated CK2β was also analyzed by SDS-PAGE and quantified by autoradiography.

CK2 subunits binding assays

MBP-CK2β-biotin (500 ng) bound to Streptavidin-coated wells was incubated in the absence or presence of CIGB-300 (50 μM). After 3 washes with Buffer A (50 mM Tris/HCl pH 7.5, 200 mM NaCl, 2% glycerol), CK2α (56 ng) was added and the CK2 activity was measured with 150 μM of peptide substrates 29 or M. Additionally, CK2α (240 ng) was incubated for 30 min at RT in the absence or presence of 100 μM CIGB-300 in streptavidin wells pre-coated with increasing amounts of CIGB-300-biotin. After 3 washes with Buffer A, CK2 activity was assayed with peptide substrate 29. For competition assays, GST-CK2α (80 ng) was incubated for 30 min at room temperature in a final volume of 15 μl in the absence or presence of 50 μM CIGB-300. After dilution in 100 μl of Buffer A, GST-CK2α was then adsorbed on Glutathione-Sepharose beads and further washed in the same buffer. Beads were finally incubated with 160 ng CK2β and CK2 activity was assayed directly on the beads with the peptide substrate M.

Pull-down assays

A total of 10×10^6 NCI-H125 cells were seeded in appropriate vessels and cultured for 18 to 20 h. Next day, the cells were trypsinized, collected by centrifugation, and lysed in hypotonic PBS solution (0.1 ×) containing 1 mM of dithiothreitol (DTT) (Sigma) and Complete protease inhibitor (Roche) by eight freeze (liquid N2)-thaw (37 °C) cycles. Then, cellular lysate was cleared by centrifugation at 12,000 rpm at 4 °C for 15 min and total protein concentration was determined by the Bradford assay (Bio-Rad). Each pull-down reaction were settled by mixing 250 μg of total protein with 100 μM of a CIGB-300-biotin-conjugated or non-conjugated CIGB-300 peptide as a competitor in a final volume of 500 μl of lysis buffer 1 ×. Subsequently, 30 μL of pre-equilibrated streptavidin-sepharose matrix (Sigma) was added to the reaction and the final reaction was incubated during 1 h at 4 °C. The matrix containing the pulled down fraction was collected by short spin, extensively washed with PBS 1 mM DTT, and analyzed by Western blotting.

Immunofluorescence and confocal microscopy

NCI-H125 cells plated on coverglass were treated with biotin-tagged CIGB-300 (50 μM) or medium alone for 10 min, 30 min, 4 h, or 24 h. Subsequently, the cells were washed with cold PBS three times and fixed in 10% formalin for 10 min at 4 °C. After permeabilization with 0.2% Triton X-100 for 10 min, cells were blocked by incubation with 4% bovine serum albumin (Sigma) in PBS for 30 min at room temperature, washed again, and incubated with rabbit polyclonal anti-CK2α (Abcam AB 10,468) 1/50 or anti-CK2β (Abcam AB151784) 1/50, or anti-nucleophosmin (B23) (Abcam AB37659) for 1 h at 37 °C. Finally, 1/200 FITC-avidin (Sigma E2761) and/or anti-rabbit-Alexa Fluor 594 (Abcam AB150080) secondary conjugates were incubated for 40 min at room temperature and washed 3 times with PBS. Coverglasses were mounted and analyzed using a Leica laser-scanning spectral Confocal microscope TCS SP8, Leica Microsystem with 20 × and 63 × objectives. Images were taken with a resolution of 1024 × 1024 Megapixels and analyzed with Leica Application Suite X (LAS X) Version 3.5.1 ($n = 5$ optical fields/variant). After conducting a normality test, a paired t-test was performed to analyze differences between Overlapping Coefficients (OC) for CK2α/CIGB-300 and B23/CIGB-300 co-localization signals.

Sample preparation for phosphoproteomic analysis

CIGB-300-treated or vehicle-treated NCI-H125 cells (two replicates) were washed with PBS and suspended in 500 μL of the lysis buffer containing 8 M urea, complete protease inhibitors (Roche, USA), phosphatase inhibitors (sodium fluoride (10 mM), sodium orthovanadate (1 mM) and sodium beta-glycerophosphate (10 mM), and 40 mM Tris/HCl, pH 8.0. After cell disruption by freeze–thaw method, samples were centrifuged at 60,000 g during 3 h and supernatants were incubated for 1 h with 10 mM DTT at 37 °C. Cysteines were modified with 25 mM acrylamide during 1 h at 25 °C. For protein enzymatic hydrolysis, samples were diluted with Tris/HCl 40 mM, pH 8.0 to decrease urea concentration up to 2 M and trypsin was added at an enzyme-to-substrate mass ratio of 1:50. Digestion proceeded for 16 h at 37 °C. Tryptic peptides were desalted by rp-HPLC and dried in a speed vac.

Phosphopeptide enrichment with TiO2 magnetic beads (MagSepharose GE)

Samples were resuspended in 1 M Glycolic acid/80% acetonitrile (ACN)/5% trifluoroacetic (TFA) and enriched for phosphopeptides with TiO2 magnetic beads following the manufacturer's instructions 28–9537-65 AB. Briefly, samples were incubated with magnetic beads under stirring (1100 rpm) for 30 min and were washed once with acid /80% ACN/5% TFA and twice with 80% ACN, 1%TFA. Non-bound and washed fractions were discarded and phosphopeptides were separated from the beads with 3 sequential elutions with NH4OH 10% under stirring (5 min, 600 rpm); eluates for each sample were pooled, rendering 1.2 mL per sample; samples were dried down in a speed vacuum centrifuge and kept at 4ºC until further analysis.

LC–MS/MS

Mass spectrometry was performed in a NanoAcquity (Waters) HPLC coupled to a LTQ Orbitrap Velos mass spectrometer (Thermo Scientific). 6.5 µL of each sample was injected and separated in a C18 reverse phase column (75 µm Øi, 25 cm, nano Acquity, 1.7 µm BEH column, Waters) using a gradient of 1 to 35% B in 120 min followed by 35–45% of B in 25 min at 250 nL/min flow rate (A: 0.1% formic acid and B: 0.1% formic acid in ACN). Eluted peptides were ionized in an emitter needle (PicoTipTM, New Objective). Spray voltage applied was 2000 V. All samples were analyzed with the multistage activation MS method (MSA) that allows for the detection of phosphopeptides.

MSA method

Data-dependent analysis was carried out in the LTQ Orbitrap Velos. Peptide masses were measured in the Orbitrap at a resolution of 60,000 (m/z: 300–1700). Up to 10 most abundant peptides (minimum intensity of 500 counts) were selected from each MS scan and fragmented using CID (38% normalized collision energy) in the linear ion trap with helium as the collision gas, and for phosphopeptide analysis, multistage activation (MSA) was enabled.

Database search and quantification

Searches were performed with MaxQuant v1.5.8.3 against SwissProt human database (2017). Missed cleavages: 2; Fixed modification: Propionamide of cysteine; variable modifications: Met oxidation and STY phosphorylation. Peptide identification was controlled at 1% FDR by target decoy method. Phosphopeptide filtering and quantification was performed using R. Phosphopeptides were filtered of reverse hits and contaminants and the sites localized with a probability ≥ 0.75 were retained. The differentially modulated phosphosites were determined by finding the difference of the mean log2(intensities) between treatment and control conditions. A phosphosite was not considered differentially modulated if the log2(intensity) values overlapped between control and treatment for any of the two replicates.

PTM database

R library iPTMnet [25] was used to retrieve phosphorylation site information and validated kinase–substrate relationships.

Sequence logo and scan

Sequence logos were generated using WebLogo V3.6.0 tool [26]. Consensus sequence scan was performed by defining R regular expressions and MaxQuant (31 amino acids) sequence window as input.

Enrichment analysis

Kinase enrichment analysis was performed using the KEA2 and PHOXTRACK tools [27, 28]. Cutoff was kept below 1% FDR. The GO ontologies and Reactome pathways enrichment analyses were performed using Enrichr [29].

Results

CIGB-300 impairs CK2 enzymatic activity in cell-free assays

To explore the possibility that CIGB-300 directly inhibits CK2 activity, the effect of CIGB-300 on the phosphorylation of two relevant CK2 peptide substrates was evaluated by a radiometric assay. Interestingly, peptide M phosphorylation, which only occurs in the presence of $CK2\alpha_2\beta_2$ holoenzyme (i.e., class-III substrate), was inhibited in a dose-dependent fashion when CIGB-300 was added to the reaction (Fig. 1a). In contrast, phosphorylation of peptide 29, whose phosphorylation can be elicited either by $CK2\alpha_2\beta_2$ or CK2α (i.e., class-I substrate), was not inhibited in this experimental setting (Fig. 1a, Fig. S1a).

Next, we tested the effect of CIGB-300 on the phosphorylation of two *bonafide* class-III substrates. In line with peptide M inhibition, CIGB-300 impaired the $CK2\alpha_2\beta_2$-dependent phosphorylation of the recombinant proteins GST-Olig2 and GST-Six1 (Fig. 1b). Otherwise, phosphorylation of Calmodulin, which is only exerted by the CK2α catalytic subunits (i.e., class-II substrate), was slightly increased in the presence of CIGB-300 (Fig. S1b). Other poly-cationic compounds exert similar disturbing effects on CK2 activity [30]. Of note, although the CK2β subunits per

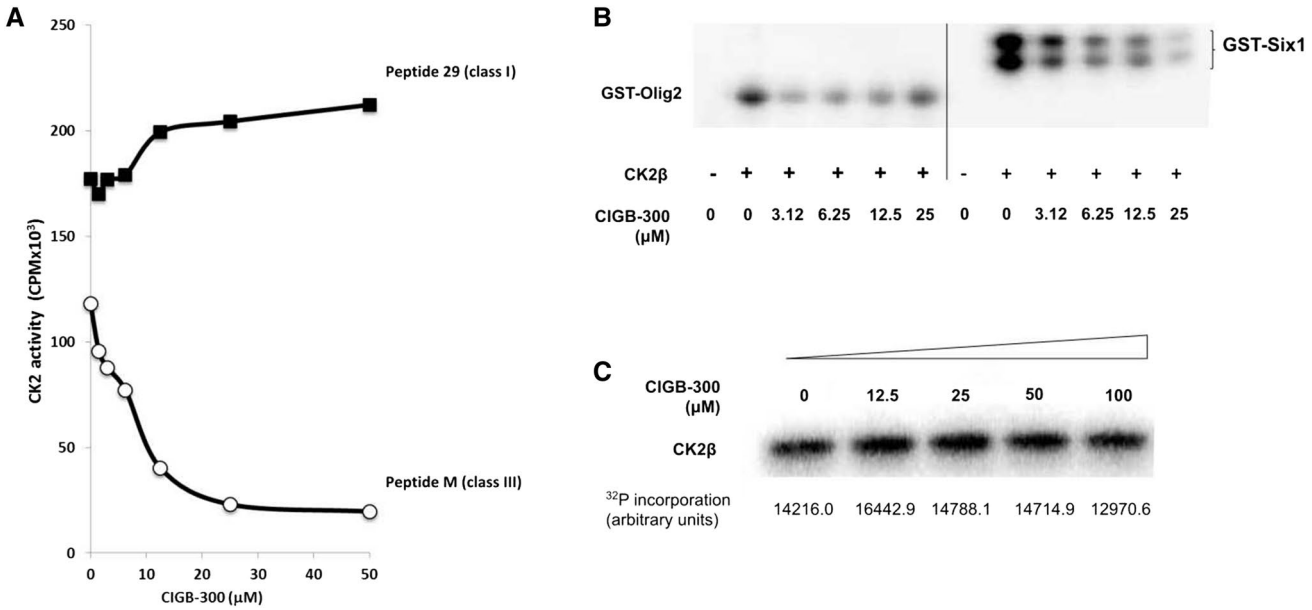

Fig. 1 Differential effects of CIGB-300 on CK2 holoenzyme activity measured by radiometric cell-free assays using recombinant enzyme subunits **a** CK2 holoenzyme (28 ng) was incubated with increasing concentrations of CIGB-300 and CK2 activity was assayed with 1 mM of peptide substrates 29 or M in a solution containing 100 mM [γ-32P]-ATP (two replicates). **b** Effect of CIGB-300 on the phosphorylation of class-III recombinant CK2 substrates or **c** on the autophosphorylation of the CK2β regulatory subunit. Phosphoproteins were analyzed by SDS-PAGE and quantified by autoradiography using Bio1D**.** Representative example of two independent experiments

se contains a CK2 consensus motif, the CIGB-300 (up to 100 μM) did not affect its phosphorylation (Fig. 1c).

CIGB-300 binds to CK2α catalytic subunit and co-localizes in situ

To understand the mechanism by which CIGB-300 impairs CK2 holoenzyme activity, we performed binding experiments and subsequent phosphorylation assays using peptide M and recombinant CK2 subunits. CK2α was incubated with increasing amounts of CK2β in the absence or presence of 100 μM CIGB-300. CK2 activity was then assayed with peptide M substrate. As expected for class-III substrates, phosphorylation of peptide M increased when increasing amounts of CK2β were added to the reaction (Fig. S2a). Such increase was almost completely abrogated in the presence of 100 μM CIGB-300, regardless of the amount of CK2β added (Fig. S2a).

Otherwise, to test for a potential CIGB-300-CK2β interaction, CK2β was immobilized on streptavidin pre-coated wells and incubated with vehicle or CIGB-300; after washing, CK2α was added and the enzymatic activity was measured by using peptide M. We found that CIGB-300 did not significantly impair subsequent holoenzyme formation nor its catalytic activity (Fig. S2b). This result suggested a lack of significant interaction between CK2β and CIGB-300. Of note, in reciprocal experiments, CIGB-300 directly interacted with CK2α when immobilized onto a solid support or in solution (Fig. 2a, b).

To corroborate CIGB-300-CK2α interaction in the cellular context, we conducted pull-down experiments using biotinylated CIGB-300 as bait to capture CK2α in cellular lysates from NCI-H125 cells. Data from Fig. 2c shows that the peptide is able to interact with CK2α, capturing roughly 90% of the total amount of the subunit present in the cellular lysate. The observed interaction is attributable to CIGB-300, since non-specific interaction between the matrix and CK2α was absent (Fig. 2c).

Furthermore, immunofluorescence microscopy analysis showed that CIGB-300 early co-localized in situ with CK2α in NCI-H125 cells. Such co-localization was mainly observed throughout the cytoplasm, with an apparent reinforcement along the perinuclear area, and to a lesser extent within the nucleus of the cell (Fig. 3, upper panel). Of note, the overall overlapping coefficient (OC) estimated from the CIGB-300-CK2α co-localization signal was above 0.5, a value only slightly below the OC measured from the CIGB-300-B23/NPM1 fluorescent signal. As previously reported, co-localization of CIGB-300 with the major target B23/NPM1 was mainly observed within the nucleolar region of the cell (Fig. 3, lower panel). CIGB-300-CK2α co-localization pattern was still evident after 4 h of peptide incubation (data not shown).

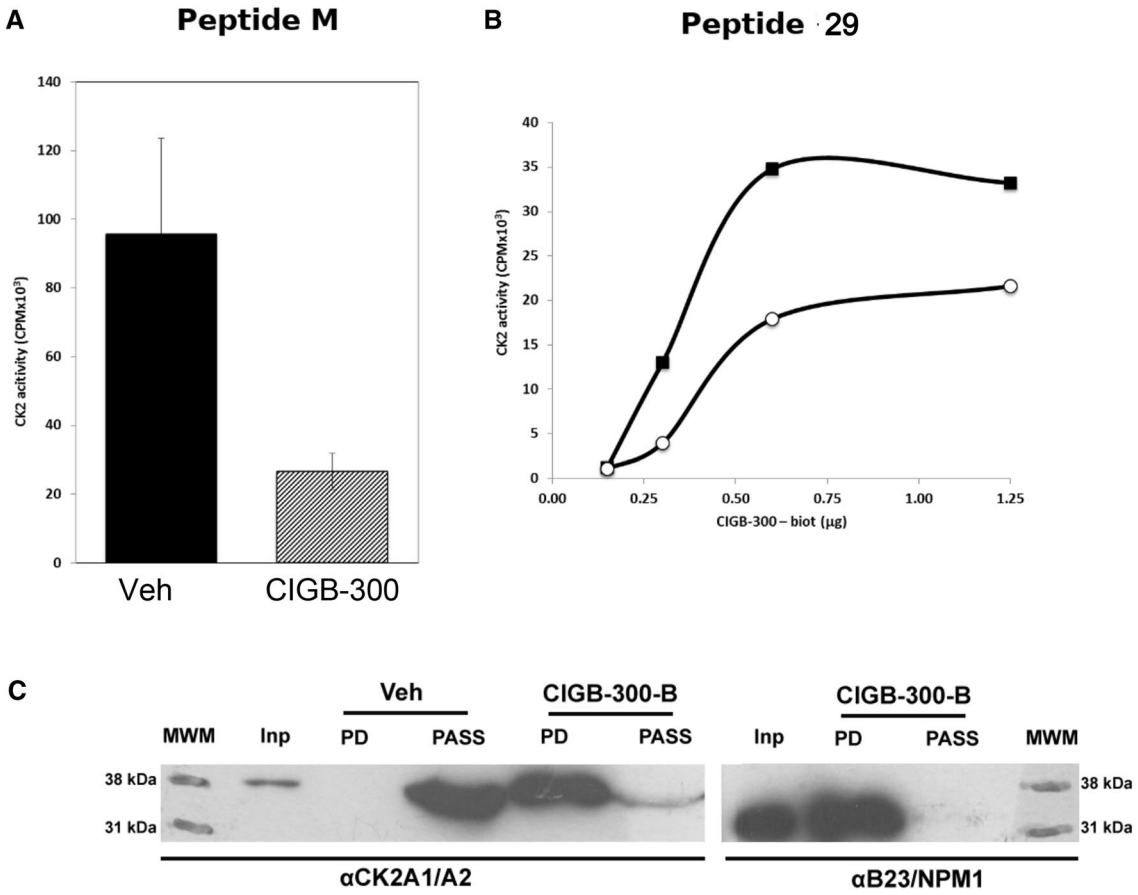

Fig. 2 Interaction of CIGB-300 with CK2α in cell-free assays or cellular lysates of NCI-H125 lung cancer cells **a** GST-CK2α (80 ng) was incubated for 30 min in the absence (black bar) or presence (hatched bar) of 50 µM CIGB-300, then the fusion protein was adsorbed on Glutathione-Sepharose beads; after washing, the beads were incubated with 160 ng CK2β and CK2 activity was assayed with peptide substrate M (two replicates) **b** CK2α (240 ng) was incubated for 30 min in the absence (■) or presence (❍) of 100 µM CIGB-300 in streptavidin wells pre-coated with increasing amounts of CIGB-300-biotin. After 3 washes, the CK2 activity was assayed with peptide substrate 29 (two replicates) **c** Pull-down experiments performed using CIGB-300-biotin as bait to capture CK2α in NCI-H125 lysates. Interacting proteins were then resolved by SDS-PAGE, transferred, and each fraction was inspected by Western blot with antibodies against $CK2\alpha_1/CK2\alpha_2$ or B23/NPM1 (control protein). Input (Inp), Vehicle (Veh), *PD* pull-down fraction, PASS: unbound fraction. Representative examples of two independent experiments

Phosphoproteomic profiling following CIGB-300 treatment of NCI-H125 cells

Our results indicate that CIGB-300 may impair CK2-mediated phosphorylation by direct enzyme inhibition in addition to substrate binding. To explore this inhibitory mechanism(s), we performed a label-free phosphoproteomic experiment in NCI-H125 cells. Unlabeled cells were treated for 10 and 30 min with either 60 µM of CIGB-300 or vehicle, lysed, and subjected to phosphopeptide enrichment and LC–MS/MS analysis. A total of 1499 phosphosites were identified across replicates corresponding to a total of 1699 proteins (including isoforms) (Fig. 4a, Table S1). From the phosphosites identified, 818 and 611 were quantified at 10 and 30 min, respectively; out of these, 476 phosphosites were shared by both time points.

Correlation between control or treatment replicates was high (≈ 0.9), whereas the correlation between control-treatment and between 10–30 min was lower (≈ 0.7), pointing to dynamic differences in the phosphoproteome (Fig. 4b). Of note, a phosphosite was deemed differentially modulated if the difference treatment–control exceeded 1.5-fold and was two-sided. Accordingly, we identified 399 (49%) and 479 (78%) phosphosites differentially inhibited at 10 min and 30 min, respectively (Fig. 4c, Table S1). Selecting a more stringent filtering criteria (i.e., threefold cutoff), we identified 42 (5%) and 232 (38%) differentially inhibited sites at 10 and 30 min, respectively (Fig.S3, Table S1). A negligible number of phosphosites were found to be differentially increased by 1.5-fold (Fig. S3, Table S1). Sequence logo analysis showed, as expected, a high frequency of inhibited phosphopeptides containing acidic residues downstream the

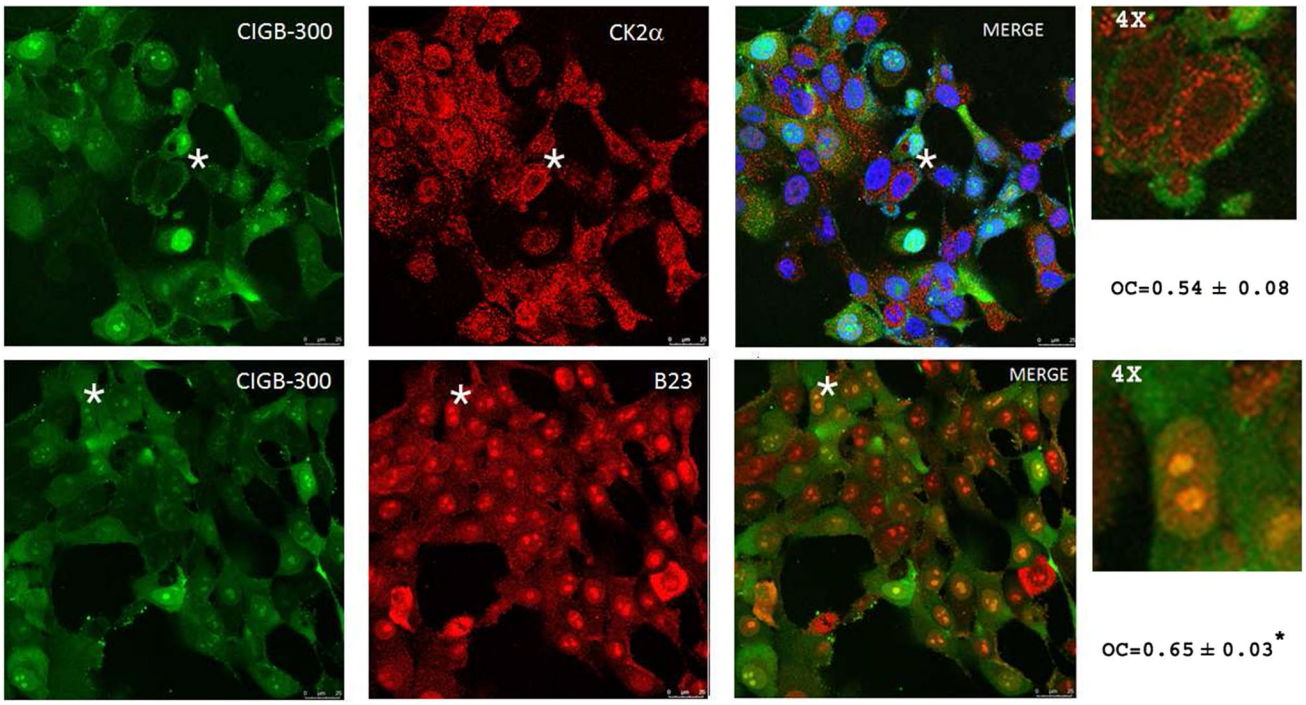

Fig. 3 CIGB-300 co-localizes in situ with CK2α in NCI-H125 cells. Representative images obtained by confocal microscopy showing the co-localization of fluorescein-conjugated-CIGB-300 with CK2α (upper panel) or with its interaction partner B23/NPM1 (lower panel) after 10 min of incubation. Representative pictures from two independent experiments. Red fluorescence: CK2/B23-derived signal; Green: CIGB-300-derived signal; Blue: nuclear DAPI; Orange: merge of Green/Red channels. Right panel, 4×magnification of the selected cell (*). OC, denotes Overlapping Coefficient as determined by Leica Application Suite X (LAS X) Version 3.5.1. * denotes *P* value < 0.05. (Color figure online)

phosphosite (Fig. 4c), in agreement with the inhibition of CK2-mediated phosphorylation. In addition, evidence for the modulation of proline-directed and basophilic kinases was shown (Fig. 4c).

Kinase–substrate relationships for differentially modulated phosphosites

A search was performed to determine which kinase–substrate relationships could be attributed to the differentially modulated phosphosites. As a result, we found 395 (out of 399) and 474 (out of 479) inhibited phosphosites at 10 and 30 min, respectively, listed in the iPTMnet database. For these, we retrieved 153 and 193 known kinase–substrate relationships corresponding to 10 and 30 min, respectively. The number of kinases represented by such relationships was 63 and 78 for 10 and 30 min, respectively (Fig. 5a, Table S2). As expected according to the sequence logo analysis and follow-up kinase enrichment analyses, the top represented kinases at both time points were CK2, PRKACA, and the proline-directed kinases CDK2, CDK1, and MAPK1 (Fig. 5b-c, Table S2). As expected, inhibition of target sites of CK2 increased from 10 to 30 min treatment but also that of PRKACA sites.

Impaired phosphorylation of CK2 substrates was observed; however, we also found a marked inhibition of CDK1/2 and PRKACA substrates. Correspondingly, we evidenced direct inhibition of phosphosites on CDK1/2/3 and on the regulatory subunits of PKA kinase: PRKAR1A and PRKAR2A. Such inhibition was marked at 30 min for PRKAR1A and PRKAR2A (Fig. 5d). The functional implications of all changes were investigated using Reactome pathway enrichment analysis (adjusted P value < 0.001, Fig. 5e, f). The Reactome pathways found mRNA splicing, gene expression, transcription, and apoptosis to be significantly enriched at both time points. Interestingly, apoptosis was found more enriched at 30 min (Fig. 5f) compared to the 10 min time point (Fig. 5e). This differential modulation of apoptosis corroborates and provides further evidence for a pro-apoptotic effect of CIGB-300 [16] (Table S2).

CIGB-300 treatment modulates CK2-dependent signaling in NCI-H125 cells

CIGB-300 treatment inhibited the phosphorylation of 8 and 10 known CK2 target sites annotated in the iPTMnet database at 10 and 30 min, respectively. Five of the phosphosites found at 10 min were also found to be inhibited at 30 min

A

Dataset	10 min	30 min
Identified phosphosites	1499	
Corresponding proteins	1699	
Quantified phosphosites	818	611
	476	
mono-phosphorylated	531	390
di-phosphorylated	271	207
tri-phosphorylated	72	56

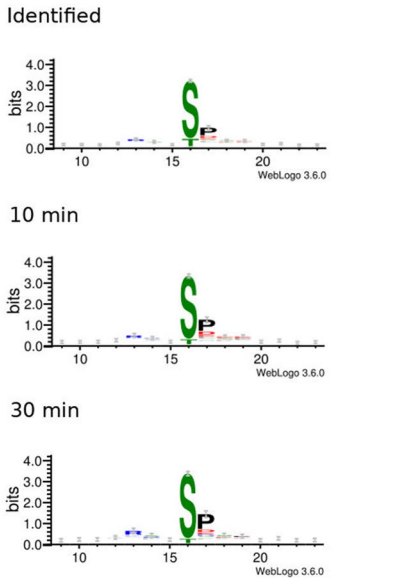

B

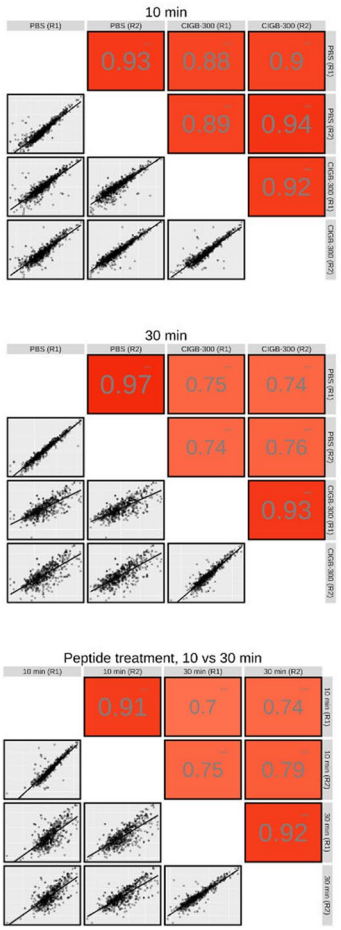

C

Inhibition	10 min	30 min
FC <= -1.5	399	479
	177	
mono-phosphorylated	295	339
di-phosphorylated	95	140
tri-phosphorylated	19	22

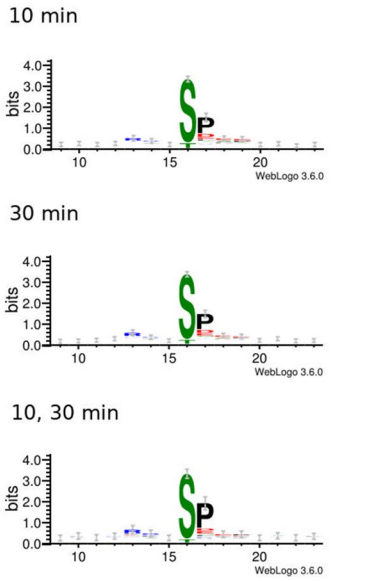

Fig. 4 Differentially inhibited phosphosites by CIGB-300 treatment of NCI-H125 cells. **a** Number of identified and quantified phosphosites at each time point and the corresponding sequence logos. The sequence logos illustrate the most frequent amino acids found at the positions surrounding the identified phosphosites or the sites quantified at 10 or 30 min, respectively. **b** Pearson correlation values observed between control and treatment samples for each replicate and between 10 and 30 min treatments with CIGB-300; *** represents a significance level of < 0.001. **c** Number of inhibited phosphosites at each time point at 1.5-fold change cutoff and the corresponding sequence logos for each time point and for overlapping sites (inhibited 10 and 30 min), respectively

(Table 1, Table S2). The majority of the changes were observed at the 30 min time point, reaching values of inhibition as lower as 20-fold. All CK2 phosphosites were found to be inhibited, except those of STMN1, which match the consensus sequence [ST][DES]x[DE] (Table 1). Given that database annotations are often incomplete, we searched the literature and scanned the sequences corresponding to the inhibited phosphosites using the CK2 consensus sequence described above. Following the literature search, Ser125 of NPM1 and Ser393 of HDAC1 were also included as modulated CK2 substrates [31, 32].

Next, a consensus sequence scan was performed and we found 64 and 75 hits at 10 and 30 min, respectively (Fig. 6a); the majority of the hits were found inhibited at 30 min. The inhibition of three of the sites Ser61 of YAP1, Ser116 of PEA15, and Ser230 of UBL7, continued to decrease markedly from 10 to 30 min reaching sixfold (Table S3). Noticeably, the phosphosites that remained unchanged at both time points or those found inhibited only at 10 min didn't match the consensus (Fig. 6a, region 3). In addition, several CK2 target sites reported in the databases conform instead to the [ST][^PRK].[DES] consensus. A scan was performed using this pattern and 28 and 34 additional sites were identified (Fig. 6b, Table S3).

Overall, ≈ 24% of the inhibited phosphosites across both time points were linked to CK2. This list was found enriched in nuclear, ribosome, and focal adhesion proteins. The biological processes and/or pathways that were found modulated in response to CIGB-300 were ribosome biogenesis, RNA processing and metabolism, chromatin

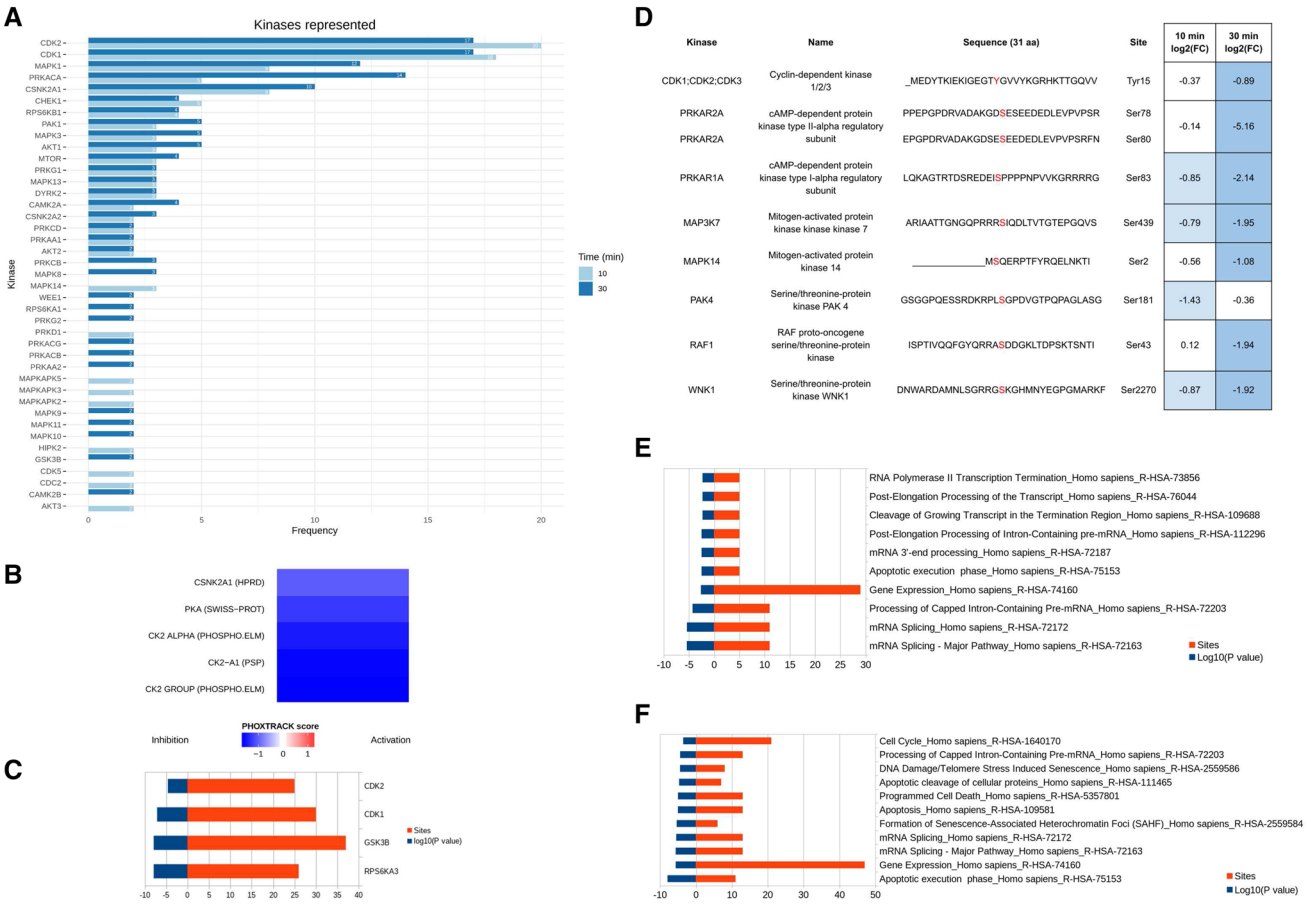

Fig. 5 Kinases modulated by CIGB-300 treatment. **a** Kinases that phosphorylate the inhibited phosphosites at 10 and/or 30 min according to the iPTMnet database. **b** Kinase enrichment analysis of phosphosites modulated at 30 min using PHOXTRACK. **c** Kinase enrichment analysis of phosphosites modulated at 30 min using KEA2. **d** Kinases containing phosphosites inhibited at 10 and/or 30 min. **e** Reactome pathways enrichment analysis of phosphosites inhibited at 10 min (adjusted P value < 0.0048). **f** Reactome pathways enrichment analysis of 30 min (adjusted P value < 0.0003)

Table 1 Known CK2 substrates differentially modulated in NCI-H125 cells by CIGB-300 treatment at 10 and/or 30 min (sites quantified in mono-phosphorylated peptides, except when stated)

Protein	Site	Sequence	10 min, log2(FC)	30 min, log2(FC)
EEF1D (P29692)	Ser162	DIDLFG**S**DNEEED	− 0.70	NA
USP7 (Q93009)	Ser18	AGEQQL**S**EPEDME	− 1.20	NA
STMN1 (P16949)	Ser16	ELEKRA**S**GQAFEL	− 1.56	− 0.63
STMN1 (P16949)	Ser63	AEERRK**S**HEAEVL	− 0.69	− 4.86
ABCF1 (Q8NE71)	Ser109	KLSVPT**S**DEEDEV	− 0.67	− 2.61
PDCD5 (O14737)	Ser119	RRKVMD**S**DEDDDY	− 0.63	− 1.77
PPP1R2 (P41236)	Ser121/Ser122	RIQEQE**SS**GEEDS	− 0.60	NA
SEPT2 (Q15019)	Ser218	HLPDAE**S**DEDEDF	− 0.61	− 4.19
HMGA1 (P17096)	Ser102/Ser103	EGISQE**SS**EEEQ_	0.1637203	− 4.614101
CDC37 (Q16543)	Ser13	WDHIEV**S**DDEDET	NA	− 2.41
MYH9 (P35579)	Ser1943	KGAGDG**S**DEEVDG	− 0.42	− 3.44
HSP90AB1 (P08238) HSP90AB2P (Q58FF8)	Ser255 Ser177	KIEDVG**S**DEEDDS	− 0.2765292	− 3.363801

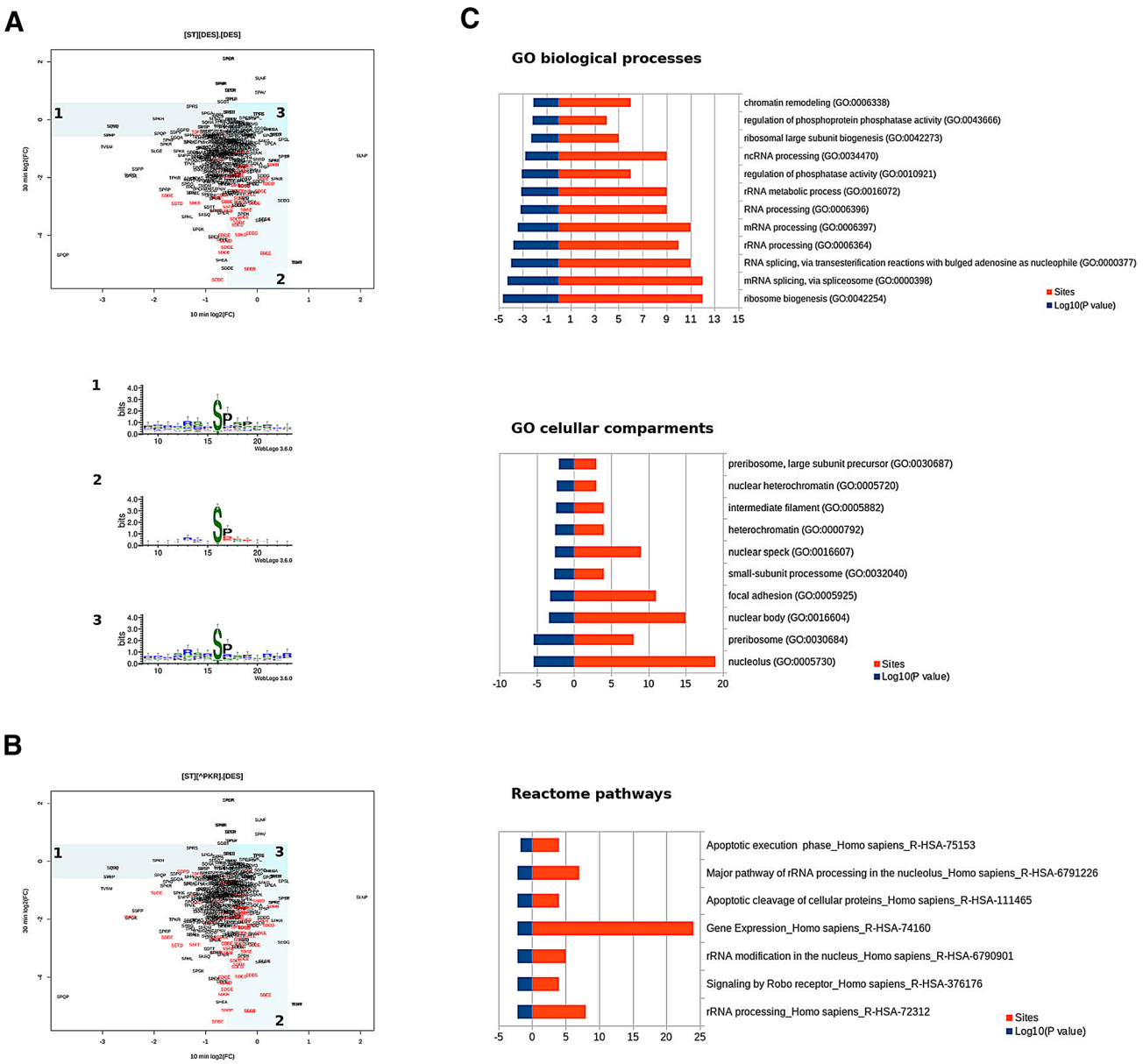

Fig. 6 Differentially inhibited phosphosites matching CK2 consensus. **a** Comparison of log2(FC) between 10 and 30 min of treatment for phosphosites matching [ST][DES]x[DES] consensus sequence. Sequence logos corresponding to regions 1, 2, and 3 of the scatter plots, respectively. **b** Similar to A for phosphosites matching [ST][PRK] × [DES] consensus sequence. **c** Gene Ontology biological processes (adjusted P value < 0.0077) and cellular compartments (adjusted P value < 0.0092) and Reactome pathway (adjusted P value < 0.0188) functional enrichment of known and predicted CK2 target sites found inhibited at one or both time points

remodeling, apoptosis, gene expression, and cell cycle (Fig. 6c).

CIGB-300 binding to CK2 phosphoacceptor sites may modulate nearby PTM sites

CK2 phosphoacceptor sites sensitive to CIGB-300 inhibition may lie in the proximity of other post-translational modifications. For instance, a kinase-substrate analysis of known CIGB-300 targets Ser129 on AKT1 and Ser380 on PTEN revealed that their direct inhibition by CIGB-300 could result in the modulation of neighboring or overlapping sites phosphorylated by other kinases and/or modified by O-Glycosyltransferases (Table S3). Therefore, these sites although significantly inhibited by CIGB-300 could be considered unintended off-targets. Of note, several of the differentially inhibited phosphosites were found to not conform the CK2 consensus sequence, but are located at a maximum distance

of 15 amino acids up or downstream the CK2 consensus sequence [ST][DES] × [DES]. Following such criterion of vicinity, we identified 42 and 62 differentially inhibited sites at 10 and 30 min, respectively (Fig. S4, Table S3). The kinase-substrate relationships found for these phosphosites pointed out to the possible unintended modulation by CIGB-300 of CHEK1, MAPK13, PAK4, CDK1, PRKACA, PRKACB, PRKACG, PRKCA, MAPK1, and MTOR signaling (Table S2). Furthermore, we found more than 95 and 140 differentially inhibited phosphosites belonging to di- or tri-phosphorylated peptides (Table S1), which suggests that for those sites targeted by CK2, the neighboring sites could also be affected.

Discussion

The CIGB-300 peptide was conceived to block CK2-mediated phosphorylation by binding to the CK2 consensus sequence present on the substrates [15]. However, since CK2β contains such a motif, it was reasonable to suspect a priori that CIGB-300 could also affect $CK2\alpha_2\beta_2$ (holoenzyme) enzymatic activity. Indeed, our cell-free assays indicated that CIGB-300 impairs $CK2\alpha_2\beta_2$-dependent (class-III) phosphorylation, but by directly binding to CK2α. Subsequent pull-down experiments demonstrated that such interaction also occurs in cellular lysates. Furthermore, the CIGB-300-CK2α interaction was corroborated in situ by con-focal microscopy throughout the cytoplasm and perinuclear region. Some nuclear co-localization was also evident, which is supported by the inhibition of nuclear localized substrates observed by mass spectrometry. Noteworthy, the CIGB-300-derived peptide chimera CRIBI-300 is also able to interact with and impair CK2 enzymatic activity in blood-derived cancer cells, further decreasing CK2α total protein levels [33].

The lack of inhibition observed for class-I (peptide 29) and class-II (calmodulin) substrates points to an exclusive inhibitory role of CIGB-300-CK2α interaction in class-III phosphorylation. Since, inhibition of CK2β phosphorylation by CIGB-300 was not observed (i.e., Substrate-binding mechanism), we hypothesize that additional determinants may be in place. Interestingly, it has been proposed that class-III phosphorylation is dependent on a CK2β acidic stretch required for substrate interaction and subsequent phosphorylation [9]. Hence we might speculate that in the context of CK2α2β2, the cationic residues from the TAT moiety of CIGB-300 could bind to this acidic stretch conferring further stability to the CIGB-300-CK2α interaction, thus preventing substrate phosphorylation. This possibility could explain the observed inhibition for recombinant class-III substrates GST-Olig2 and GST-Six1 and the lack of inhibition for class-I and -II. Altogether, these findings point out to a potential additional mechanism by which CIGB-300 could directly impact CK2 activity in cancer cells.

To identify the full array of CK2 substrates impaired by CIGB-300, we conducted a phosphoproteomic analysis in NCI-H125 lung cancer cells. Our results indicated that CIGB-300 treatment induces a marked inhibition of the phosphoproteome; 41 and 78% of the phosphosites quantified at 10 and 30 min, respectively. The percentage of known and candidate CK2 substrates inhibited at either time point was 24%. Moreover, a significant number of apparently unrelated phosphosites found inhibited were linked to proteins containing CK2 consensus and/or as substrates of kinases regulated by CK2, thus reflecting the complexity of inhibitory events triggered by CIGB-300 in cancer cells. Several known CK2 substrates were identified as CIGB-300 targets including Ser125 of B23/NPM1, which corroborates a main target of CIGB-300 previously identified by our group [16]. Overall the processes modulated were translation, ribosome biogenesis [34], apoptosis [35, 36], protein folding [37, 38], cytoskeleton reorganization [39, 40], protein ubiquitination [41], and microtubule formation [42]. Interestingly, a BAD-dependent mechanism by which CIGB-300 could mediate its pro-apoptotic effect emerged from our analysis based on the inhibition observed at Ser118 of BAD and at the CK2 target sites Ser78 and Ser80 of PRKAR2A. Accordingly, inhibition of PRKAR2A by CIGB-300 could result in an impairment of PKA activity and in turn a differential inhibition of Ser118 of BAD, thus promoting BAD's pro-apoptotic function [43, 44]. This finding further emphasizes the intricate interplay among the different kinases which operates in a cell [45]. Concerning off-target events, we should note that binding of CIGB-300 to phosphoacceptor sites on a protein substrate may impair nearby phosphorylation sites by steric hindrance or induced conformational changes.

Overall, no distinction could be made regarding which mechanism of CK2 inhibition prevailed on NCI-H125 cells once incubated with CIGB-300. However, we observed the inhibition of Ser162 on EEF1D, a class-I substrate, and previously identified CIGB-300-interactor in a pull-down experiment in NCI-H125 cells (*unpublished data*). Thus, our findings point to EEF1D as a candidate for inhibition mediated by direct substrate binding. EEF1D is a *bonafide* CK2 substrate which contains a highly acidic sequence, similar to the CK2 target region initially used for the isolation of the CIGB-300 peptide [15]. On the other hand, Ser2 of EIF2s2 from which peptide M was derived was not found inhibited by CIGB-300 in our experimental conditions. Inhibition of Ser2 residue of EIF2s2 by the CX-4945 has been reported in mitotic HeLa cells [37], thus indicating divergences among CIGB-300 and CX-4945 mechanism of action in cancer cells.

The phosphoproteomics study in mitotic-arrested HeLa cells further describes the biological processes and substrates

modulated by CX-4945 [46]. This study provides a comprehensive list of CX-4945 responsive sites and highlights its potential off-target effects. Equally important, it informs on the extensive impact on the phosphoproteome of this clinically relevant CK2 inhibitor, with more than 400 sites reported to be inhibited. The list of inhibited phosphosites includes previously validated sites from known CK2 substrates such as EIF2s2 (EIF2β), EEF1D, HDAC1, HDAC2, HSP90AA1, and PPP1R2 [46]. Our results only partially recapitulated those observed after CX-4945 treatment with 12 inhibited CK2 substrates and 8 differentially inhibited phosphosites in common (i.e., EEF1Ds162; SRRM1s874; ABCF1s109; DKC1s451; PRCCs159; NOP58s502; GBF1s1319 and IWS1s398). Overall, we observed key differences concerning the number, identity, and extension of CK2 substrates inhibited by these drugs. Another phosphoproteomic analysis was done with the inhibitor quinalizarin on HEK293 cells [47]. The CK2 substrates AKAP12, SRRM1, ZRANB2, LARP7, IWS1, BCLAF1, and PPP1R2 were identified in common as inhibited by quinalizarin and CIGB-300 under the experimental conditions tested. Of note, besides the actual mechanistic differences between CIGB-300 and these other two CK2 inhibitors, the experimental approach and the cellular models used could also be contributed to the observed differences.

Studies have shown aberrant CK2 activity in cancer compared to normal cells, suggesting that malignant cells are addicted to CK2 activity [2]. The finding that CK2 consensus motif is widespread in the human proteome [48] and the known functional pleiotropy of CK2 subunits [49] have long raised concerns regarding the safety of therapies targeting CK2. However, both CIGB-300 and CX-4945 inhibitors have proven to be safe and well tolerated in humans [13, 14]. The repertoire of CK2 substrate inhibited by CIGB-300 described here provides a molecular basis for its in vitro and in vivo anti-neoplastic effects. Further experimental validation needs to be performed in order to identify those CK2-related and non-CK2-related events suitable as CIGB-300 response biomarkers. Interestingly, phosphorylation by other kinases involved in several hallmarks of cancer was also impaired by CIGB-300. This potential multitarget pharmacological effect along with the favorable risk–benefit balance already observed in clinical trials, supports CIGB-300 as a promising drug candidate to be tested in unmet oncology settings like advanced and/or chemo-refractory cancer.

Funding This work was conducted with the financial support of the CIGB-300 Grant, Biomedical Research Division, CIGB, Cuba.

Compliance with ethical standards

Conflict of interest The authors declare that they have no conflict of interest.

References

1. Salvi M, Cesaro L, Pinna LA (2010) Variable contribution of protein kinases to the generation of the human phosphoproteome: a global weblogo analysis. Biomol Concepts 1(2):185–195. https://doi.org/10.1515/bmc.2010.013
2. Ruzzene M (1804) Pinna LA (2010) Addiction to protein kinase CK2: A common denominator of diverse cancer cells? Biochim Biophys Acta (BBA) Proteins Proteom 3:499–504
3. Barata JT (2011) The impact of PTEN regulation by CK2 on PI3K-dependent signaling and leukemia cell survival. Adv Enzyme Regul 51(1):37–49. https://doi.org/10.1016/j.advenzreg.2010.09.012
4. Scaglioni PP, Yung TM, Cai LF et al (2006) A CK2-dependent mechanism for degradation of the PML tumor suppressor. Cell 126:269–283
5. Di Maira G, Salvi M, Arrigoni G et al (2005) Protein kinase CK2 phosphorylates and upregulates Akt/PKB. Cell Death Differ 12:668–677
6. Channavajhala PL, Seldin DC (2002) Functional interaction of protein kinase CK2 and c-Myc in lymphogenesis. Oncogene 21:5280–5288
7. Chua MMJ, Ortega CE, Sheikh A et al (2017) CK2 in Cancer: cellular and biochemical mechanisms and potential therapeutic target. Pharmaceuticals 10:18. https://doi.org/10.3390/ph10010018
8. Pinna LA (2002) Protein kinase CK2: a challenge to canons. J Cell Sci 115:3873–3878
9. Nunez de Villavicencio-Diaz T, Mazola Y, Perera Negrin Y et al (2015) Predicting CK2 beta-dependent substrates using linear patterns. Biochem Biophys Rep 4:20–27. https://doi.org/10.1016/j.bbrep.2015.08.011
10. Siddiqui-Jain A, Drygin D, Streiner N et al (2010) CX-4945, an orally bioavailable selective inhibitor of protein kinase CK2, inhibits prosurvival and angiogenic signaling and exhibits antitumor efficacy. Can Res 70(24):10288–10298. https://doi.org/10.1158/0008-5472.CAN-10-1893
11. Laudet B, Barette C, Dulery V et al (2007) Structure-based design of small peptide inhibitors of protein kinase CK2 subunit interaction. Biochem J 408(3):363–373. https://doi.org/10.1042/BJ20070825
12. Slaton JW, Unger GM, Sloper DT, Davis AT, Ahmed K (2004) Induction of apoptosis by antisense CK2 in human prostate cancer xenograft model. Mol Cancer Res 2(12):712–721
13. Marschke RF, Borad MJ, McFarland RW et al (2011) Findings from the phase I clinical trials of CX-4945, an orally available inhibitor of CK2. J Clin Oncol 29:3087. https://doi.org/10.1200/jco.2011.29.15_suppl.3087
14. Solares AM, Santana A, Baladrón I et al (2009) Safety and preliminary efficacy data of a novel Casein Kinase 2 (CK2) peptide inhibitor administered intralesionally at four dose levels in patients with cervical malignancies. BMC Cancer 9:146
15. Perea SE, Reyes O, Puchades Y et al (2004) Antitumor effect of a novel proapoptotic peptide that impairs the phosphorylation by the protein kinase 2 (casein kinase 2). Can Res 64(19):7127–7129. https://doi.org/10.1158/0008-5472.CAN-04-2086
16. Perera Y, Farina HG, Gil J et al (2009) Anticancer peptide CIGB-300 binds to nucleophosmin/B23, impairs its

CK2-mediated phosphorylation, and leads to apoptosis through its nucleolar disassembly activity. Mol Cancer Ther 8(5):1189–1196. https://doi.org/10.1158/1535-7163.MCT-08-1056
17. Perea SE, Baladron I, Garcia Y et al (2011) CIGB-300, a synthetic peptide-based drug that targets the CK2 phosphoaceptor domain. Translational and clinical research. Mol Cell Biochem 356:45–50. https://doi.org/10.1007/s11010-011-0950-y
18. Martins LR, Perera Y, Lucio P et al (2014) Targeting chronic lymphocytic leukemia using CIGB-300, a clinical-stage CK2-specific cell-permeable peptide inhibitor. Oncotarget 5(1):258–263. https://doi.org/10.18632/oncotarget.1513
19. Boldyreff B, James P, Staudenmann W, Issinger OG (1993) Ser2 is the autophosphorylation site in the beta subunit from bicistronically expressed human casein kinase-2 and from native rat liver casein kinase-2 beta. Eur J Biochem 218(2):515–521. https://doi.org/10.1111/j.1432-1033.1993.tb18404.x
20. Litchfield DW, Lozeman FJ, Cicirelli MF et al (1991) Phosphorylation of the beta subunit of casein kinase II in human A431 cells. Identification of the autophosphorylation site and a site phosphorylated by p34cdc2. J Biol Chem 266(30):20380–20389
21. Pagano MA, Sarno S, Poletto G et al (2005) Autophosphorylation at the regulatory beta subunit reflects the supramolecular organization of protein kinase CK2. Mol Cell Biochem 274:23–29. https://doi.org/10.1007/s11010-005-3116-y
22. Zhang C, Vilk G, Canton DA, Litchfield DW (2002) Phosphorylation regulates the stability of the regulatory CK2beta subunit. Oncogene 21(23):3754–3764. https://doi.org/10.1038/sj.onc.1205467
23. Rodriguez-Ulloa A, Ramos Y, Gil J et al (2010) Proteomic profile regulated by the anticancer peptide CIGB-300 in non-small cell lung cancer (NSCLC) cells. J Proteome Res 9(10):5473–5483. https://doi.org/10.1021/pr100728v
24. Leroy D, Filhol O, Quintaine N et al (1999) Dissecting subdomains involved in multiple functions of the CK2beta subunit. Mol Cell Biochem 191:43–50
25. Huang H, Arighi CN, Ross KE et al (2018) iPTMnet: an integrated resource for protein post-translational modification network discovery. Nucleic Acids Res 46:D542–D550. https://doi.org/10.1093/nar/gkx1104
26. Crooks GE, Hon G, Chandonia JM, Brenner SE (2004) WebLogo: a sequence logo generator. Genome Res 14(6):1188–1190. https://doi.org/10.1101/gr.849004
27. Lachmann A, Ma'ayan A (2009) KEA: kinase enrichment analysis. Bioinformatics 25(5):684–686. https://doi.org/10.1093/bioinformatics/btp026
28. Weidner C, Fischer C, Sauer S (2014) PHOXTRACK-a tool for interpreting comprehensive datasets of post-translational modifications of proteins. Bioinformatics 30(23):3410–3411. https://doi.org/10.1093/bioinformatics/btu572
29. Kuleshov MV, Jones MR, Rouillard AD et al (2016) Enrichr: a comprehensive gene set enrichment analysis web server 2016 update. Nucleic Acids Res 44(W1):W90–97. https://doi.org/10.1093/nar/gkw377
30. Romero-Oliva F, Jacob G, Allende JE (2003) Dual effect of lysine-rich polypeptides on the activity of protein kinase CK2. Cell Biochem 89(2):348–355
31. Szebeni A, Hingorani K, Negi S, Olson MOJ (2003) Role of protein kinase CK2 phosphorylation in the molecular chaperone activity of nucleolar protein b23. J Biol Chem 278(11):9107–9115. https://doi.org/10.1074/jbc.M204411200
32. Adenuga D, Rahman I (2010) Protein kinase CK2-mediated phosphorylation of HDAC2 regulates co-repressor formation, deacetylase activity and acetylation of HDAC2 by cigarette smoke and aldehydes. Arch Biochem Biophys 498(1):62–73. https://doi.org/10.1016/j.abb.2010.04.002
33. Zanin S, Sandre M, Cozza G et al (2015) Chimeric peptides as modulators of CK2-dependent signaling: Mechanism of action and off-target effects. Biochem Biophys Acta 1854:1694–1707. https://doi.org/10.1016/j.bbapap.2015.04.026
34. Paytubi S, Wang X, Lam YW et al (2009) ABC50 promotes translation initiation in mammalian cells. J Biol Chem 284(36):24061–24073. https://doi.org/10.1074/jbc.M109.031625
35. Salvi M, Xu D, Chen Y (2009) Programmed cell death protein 5 (PDCD5) is phosphorylated by CK2 in vitro and in 293T cells. Biochem Biophys Res Commun 387(3):606–610. https://doi.org/10.1016/j.bbrc.2009.07.067
36. Li G, Ma D (1863) Chen Y (2016) Cellular functions of programmed cell death 5. Biochem Biophys Acta 4:572–580. https://doi.org/10.1016/j.bbamcr.2015.12.021
37. Miyata Y, Nishida E (2004) CK2 controls multiple protein kinases by phosphorylating a kinase-targeting molecular chaperone, Cdc37. Mol Cell Biol 24(9):4065–4074. https://doi.org/10.1128/mcb.24.9.4065-4074.2004
38. Kim SW, Hasanuzzaman M, Cho M et al (2015) Casein Kinase 2 (CK2)-mediated phosphorylation of Hsp90beta as a novel mechanism of rifampin-induced MDR1 expression. J Biol Chem 290(27):17029–17040. https://doi.org/10.1074/jbc.M114.624106
39. Betapudi V, Gokulrangan G, Chance MR, Egelhoff TT (2011) A proteomic study of myosin II motor proteins during tumor cell migration. J Mol Biol 407(5):673–686. https://doi.org/10.1016/j.jmb.2011.02.010
40. Yu W, Ding X, Chen F et al (2009) The phosphorylation of SEPT2 on Ser218 by casein kinase 2 is important to hepatoma carcinoma cell proliferation. Mol Cell Biochem 325:61–67. https://doi.org/10.1007/s11010-008-0020-2
41. Khoronenkova SV, Dianova II, Ternette N et al (2012) ATM-dependent downregulation of USP7/HAUSP by PPM1G activates p53 response to DNA damage. Mol Cell 45(6):801–813. https://doi.org/10.1016/j.molcel.2012.01.021
42. Moreno FJ, Avila J (1998) Phosphorylation of stathmin modulates its function as a microtubule depolymerizing factor. Mol Cell Biochem 183:201–209. https://doi.org/10.1023/a:1006807814580
43. Polzien L, Baljuls A, Rennefahrt UEE et al (2009) Identification of novel in vivo phosphorylation sites of the human proapoptotic protein BAD: pore-forming activity of BAD is regulated by phosphorylation. J Biol Chem 284(41):28004–28020. https://doi.org/10.1074/jbc.M109.010702
44. Bui NLC, Pandey V, Zhu T, Ma L, Basappa Lobie PE (2018) Bad phosphorylation as a target of inhibition in oncology. Cancer Lett 415:177–186. https://doi.org/10.1016/j.canlet.2017.11.017
45. St-Denis N, Gabriel M, Turowec JP et al (2015) Systematic investigation of hierarchical phosphorylation by protein kinase CK2. J Proteom 118:49–62. https://doi.org/10.1016/j.jprot.2014.10.020
46. Rusin SF, Adamo ME, Kettenbach AN (2017) Identification of candidate casein kinase 2 substrates in mitosis by quantitative phosphoproteomics. Front Cell Dev Biol 5:97. https://doi.org/10.3389/fcell.2017.00097
47. Franchin C, Cesaro L, Salvi M et al (1854) (2015) Quantitative analysis of a phosphoproteome readily altered by the protein kinase CK2 inhibitor quinalizarin in HEK-293T cells. Biochim Biophys Acta 6:609–623. https://doi.org/10.1016/j.bbapap.2014.09.017
48. Salvi M, Sarno S, Cesaro L, Nakamura H, Pinna LA (2009) Extraordinary pleiotropy of protein kinase CK2 revealed by weblogo phosphoproteome analysis. Biochem Biophys Acta 1793(5):847–859. https://doi.org/10.1016/j.bbamcr.2009.01.013
49. Franchin C, Borgo C, Zaramella S et al (2017) Exploring the CK2 paradox: restless, dangerous, dispensable. Pharmaceuticals 10(1):11. https://doi.org/10.3390/ph10010011